Oxidation and reduction of pyridine nucleotides in alamethicin-permeabilized plant mitochondria

Fredrik I. JOHANSSON*, Agnieszka M. MICHALECKA*, Ian M. MØLLER† and Allan G. RASMUSSON*[1]

*Department of Cell and Organism Biology, Lund University, Sölvegatan 35B, SE-223 62 Lund, Sweden, and †Plant Research Department, Risø National Laboratory, Building 301, P.O. Box 49, DK-4000 Roskilde, Denmark

The inner mitochondrial membrane is selectively permeable, which limits the transport of solutes and metabolites across the membrane. This constitutes a problem when intramitochondrial enzymes are studied. The channel-forming antibiotic AlaM (alamethicin) was used as a potentially less invasive method to permeabilize mitochondria and study the highly branched electron-transport chain in potato tuber (*Solanum tuberosum*) and pea leaf (*Pisum sativum*) mitochondria. We show that AlaM permeabilized the inner membrane of plant mitochondria to NAD(P)H, allowing the quantification of internal NAD(P)H dehydrogenases as well as matrix enzymes *in situ*. AlaM was found to inhibit the electron-transport chain at the external Ca^{2+}-dependent rotenone-insensitive NADH dehydrogenase and around complexes III and IV. Nevertheless, under optimal conditions, especially complex I-mediated NADH oxidation in AlaM-treated mitochondria was much higher than what has been previously measured by other techniques. Our results also show a difference in substrate specificities for complex I in mitochondria as compared with inside-out submitochondrial particles. AlaM facilitated the passage of cofactors to and from the mitochondrial matrix and allowed the determination of NAD^+ requirements of malate oxidation *in situ*. In summary, we conclude that AlaM provides the best method for quantifying NADH dehydrogenase activities and that AlaM will prove to be an important method to study enzymes under conditions that resemble their native environment not only in plant mitochondria but also in other membrane-enclosed compartments, such as intact cells, chloroplasts and peroxisomes.

Key words: alamethicin, complex I, electron-transport chain, NADH dehydrogenase, permeabilization, plant mitochondria.

INTRODUCTION

Mitochondria contain an outer and an inner membrane. The outer membrane has pores that are freely permeable to molecules smaller than approx. 10 kDa. Therefore the intermembrane space has the same composition as the cytosol with respect to low-molecular-mass compounds [1]. The outer membrane surrounds the highly invaginated inner membrane, which makes up the osmotic barrier and forms a tightly sealed compartment by enclosing the matrix. The inner membrane is selectively permeable, so transport of solutes and metabolites, e.g. malate, succinate and NAD^+, takes place with the help of specific transport proteins. For some solutes, e.g. NAD(P)H, there appear to be no transporters and consequently they do not pass the membrane at a rate relevant for enzymic assays of intramitochondrially located enzymes' activities. Techniques to overcome this problem include treatment with detergents, osmotical disruption and subfractionation after disruption by sonication. These techniques release and dilute the matrix content and may affect the native membrane structure and the enzyme environment, which may damage the ETC (electron-transport chain). Also, matrix enzyme complexes, e.g. glycine decarboxylase, dissociate after mitochondrial rupture and matrix dilution. This complicates the study of several enzymes and complexes, for example determination of tissue enzyme capacities in response to environmental cues or perturbations of function by transgenes. Therefore more direct methods are needed for measuring accurately the enzymes enclosed by the inner-membrane barrier.

A less invasive method to get access to the inner side of the inner mitochondrial membrane is the use of the antibiotic AlaM (alamethicin). AlaM is a 20-residue channel-forming peptide from the fungus *Trichoderma viride*. The AlaM molecule is α-helical in conformation, which is stabilized by the presence of a large number of aminoisobutyric acid residues. After insertion into a membrane, the peptide forms a voltage-dependent channel with a helix bundle surrounding a central pore [2]. AlaM channels show a multiconductance behaviour where the difference in conductance level corresponds to different numbers of peptides in the pore complex. The pore complex is made up of a variable number of monomers ($3–4 < N < 12$) because of uptake and release of peptide monomers [3]. In mammalian mitochondria, the channels allow the passage of low-molecular-mass compounds such as ATP, ADP and NADH [4,5], but retain larger compounds such as soluble matrix proteins [5,6]. In rat liver and heart mitochondria, AlaM has been shown to allow access for NADH to the internal rotenone-sensitive NADH dehydrogenase (complex I) [5–7].

The mitochondrial ETC is more complex in plants when compared with that in mammals. In addition to the ubiquitous rotenone-sensitive NADH dehydrogenase, complex I (EC 1.6.5.3), there are four separate non-proton-pumping rotenone-insensitive NAD(P)H dehydrogenases in the plant ETC [8,9]. Matrix NADH can be oxidized by either complex I or an ND_{in}(NADH) (internal rotenone-sensitive NADH dehydrogenase) [10,11]. Furthermore, a Ca^{2+}-dependent rotenone-insensitive NADPH dehydrogenase is present on the matrix surface of the inner membrane [12,13]. Cytosolic NADH can be oxidized by an external Ca^{2+}-dependent

Abbreviations used: AlaM, alamethicin; DaNADH, deamino-NADH; DcQ, decylubiquinone; DQH_2, duroquinol; ETC, electron-transport chain; IO-SMP, inside-out submitochondrial particles; MDH, malate dehydrogenase; ND_{ex}(NADH), external rotenone-insensitive NADH dehydrogenase; ND_{in}(NADH), internal rotenone-insensitive NADH dehydrogenase; PLM, pea leaf mitochondria; POM, potato tuber mitochondria.

[1] To whom correspondence should be addressed (e-mail allan.rasmusson@cob.lu.se).

ND_{ex}(NADH) (external rotenone-insensitive NADH dehydrogenase). Also the external NADPH is oxidized in a Ca^{2+}-dependent manner [14,15]. Whereas the external enzymes are easily measured in isolated mitochondria, the internal enzymes are hidden within the inner membrane.

In the present study, we show that AlaM permeabilizes the inner membrane of plant mitochondria to NAD(P)H and allows the measurement of the internal NAD(P)H dehydrogenases directly, as well as coupled with matrix enzymes *in situ*. Additionally, AlaM inhibits the ETC at the ND_{ex}(NADH) and around complexes III and IV, an inhibition not observed previously. A comparison between NADH oxidation in IO-SMP (inside-out submitochondrial particles) and in osmotically disrupted and AlaM-treated POM (potato tuber mitochondria) shows that AlaM provides the best method for quantifying NADH dehydrogenase activities. Interestingly, complex I has different pyridine nucleotide specificity depending on the assay system used.

MATERIALS AND METHODS

Plant material and preparation of mitochondrial fractions

Potato (*Solanum tuberosum* L. cv. Bintje) tubers were purchased from the local market. POM and IO-SMP were isolated as described in [16] and [11] respectively.

Pea (*Pisum sativum* L. cv. Oregon) plants were grown in trays with vermiculite for 14 days in a greenhouse at 20 °C, 50–55 % relative humidity, with a photoperiod of 16 h light (200 μmol $\cdot$ m^{-2} $\cdot$ s^{-1}) per day. PLM (pea leaf mitochondria) were isolated from green leaves as described in [17].

Purified mitochondria were frozen in liquid nitrogen after addition of 5 % (v/v) DMSO and stored at − 80 °C until used. As a control, the results in Figure 3(c) were reproduced on freshly prepared mitochondria with virtually identical results. The protein concentration was determined by the bicinchoninic acid reagent according to the manufacturer's instructions (Sigma, St. Louis, MO, U.S.A.). The protein content of PLM was corrected for the contribution by broken thylakoids by assuming a thylakoid protein to chlorophyll mass ratio of 7 [18]. Chlorophyll was determined by the method of Arnon [19].

Oxygen consumption

Respiration was measured as oxygen consumption in a Clark Oxygen Electrode (Rank Brothers, Cambridge, U.K.) at 25 °C. For POM and IO-SMP the reaction medium contained 0.3 M sucrose, 10 mM Mops, 2.5 mM $MgCl_2$ and 0.5 mM EGTA (pH 7.2). For PLM the reaction medium contained 0.3 M mannitol, 10 mM Mops, 2.5 mM $MgCl_2$ and 0.5 mM EGTA (pH 7.2). The uncoupler carbonyl cyanide *p*-trifluoromethoxyphenylhydrazone was added to the reaction medium to a concentration of 0.4 μM in all the measurements except when malate was used as substrate. The cytochrome pathway was inhibited by the addition of 0.4 μM antimycin A.

The concentrations of NADH, NADPH and DaNADH (deamino-NADH) were 1 mM in the assays. During NAD(P)H and DaNADH oxidation, 20 μM rotenone was added to the assay mixture to inhibit complex I, and 1 mM $CaCl_2$ was subsequently added to activate Ca^{2+}-dependent NAD(P)H dehydrogenases.

DQH_2 (duroquinol) was dissolved in DMSO and the solution was bubbled with N_2 and kept under N_2 to avoid autoxidation. The final concentration of DQH_2 in the reaction medium was 1 mM. The antimycin A-insensitive part of the DQH_2 oxidation was never above 10 % and was subtracted from the DQH_2 oxidation rates.

Succinate oxidation was measured with 10 mM succinate in the assay in the presence of 0.5 mM ATP to activate succinate dehydrogenase. The protein concentration was 80 μg/ml. Malate oxidation was measured with 10 mM malate in the assay in the presence of 0.5 mM CoA and 10 mM glutamate. Activities were measured after each subsequent addition of malate, 0.25 mM ADP and NAD^+ (0.025–2 mM as indicated), the latter added in state 3. Malate oxidation was corrected for antimycin A-insensitive rate (< 5 % of maximum activity), which was probably due to baseline drift in the oxygen electrode.

Osmotic disruption of mitochondria

Osmotic disruption of POM was performed in a medium containing 1 mM Mops, 0.105 mM EGTA (pH 7.2) for 6 min at room temperature (25 °C) to permeabilize the inner membrane [20]. The suspension was then supplemented with Mops, $MgCl_2$ and EGTA to make up the assay medium for POM without sucrose and the reaction was started by addition of NADH. Where indicated, cytochrome *c* was added to the burst mitochondria at a final concentration of 5 μM.

Spectrophotometric enzyme assays

Complex IV (EC 1.9.3.1) activity was determined in terms of cytochrome *c* oxidation as described by Rasmusson and Møller [21]. NAD^+-dependent MDH (malate dehydrogenase, EC 1.1.1.37) was determined as described by Møller et al. [22]. In both the cases Triton X-100 was added at a final concentration of 0.025 % (w/v) to measure the total activity. The POM were intact, as indicated by 90 and 96 % latency of complex IV and MDH respectively. The complex IV latency of the IO-SMP was 90 %, indicating that at most 10 % of the submitochondrial particles were right-side-out (results not shown).

NADH oxidation with DcQ (decylubiquinone) as electron acceptor was measured spectrophotometrically at dual wavelength (340–400 nm) in the same medium as for POM O_2 consumption using 20 μM DcQ and with 0.4 μM antimycin A additionally present to inhibit complex III. NADH was added at a concentration of 0.1 mM to the reaction medium and the decrease in NADH concentration was measured.

General techniques

All enzyme activities were measured in the presence and absence of AlaM. AlaM (Sigma) was dissolved in ethanol to a concentration of 10 mg/ml in the stock solution and stored at − 20 °C. In the measurements, AlaM was added to a final concentration of 2–60 μg/ml as indicated. Ethanol was never above 0.8 % (v/v) in any assay.

Results presented are from representative experiments. Similar results were obtained from at least two independent preparations.

RESULTS

AlaM makes the inner mitochondrial membrane permeable to NADH and NADPH

The ability of AlaM to permeabilize the inner membrane of intact POM to NADH, malate and oxaloacetate was studied by measuring the activity of the matrix enzyme NAD^+-MDH. Figure 1 shows that increasing concentrations of AlaM led to increased NADH-dependent MDH activity, which reached a maximum above an AlaM concentration of 38 μg/ml. In the presence of the detergent Triton X-100, which releases all the MDH to the assay mixture, the activity remained unaffected by

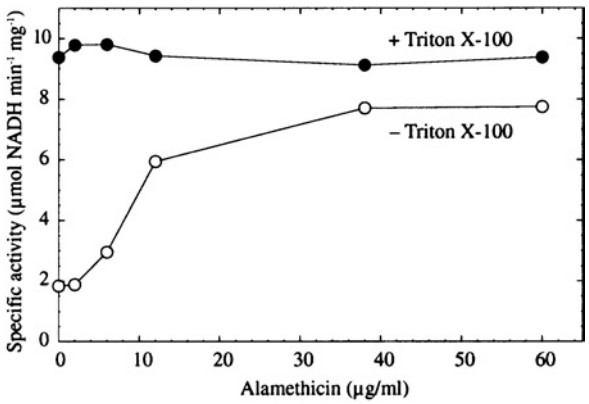

Figure 1 NADH-dependent MDH activity in POM as a function of AlaM concentration

Activity was measured in the presence (●) or absence (○) of the detergent Triton X-100. The protein concentration in the assay was 1 μg/ml.

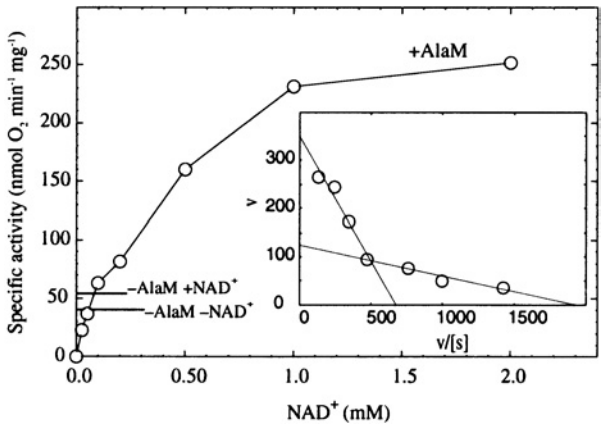

Figure 2 Malate oxidation by POM in the presence of 22 μg/ml AlaM as a function of NAD$^+$ concentration in the medium

The activities were measured in the presence of ADP. The malate oxidation in intact mitochondria (without AlaM) was 54 and 40 nmol of $O_2 \cdot min^{-1} \cdot (mg\ of\ protein)^{-1}$ in the presence (− AlaM + NAD$^+$) or absence (− AlaM − NAD$^+$) of 0.5 mM NAD$^+$ respectively, as indicated by horizontal lines in the Figure. The concentration of mitochondria was 80 μg of protein/ml. Inset: same activities in an Eadie–Hofstee plot with linear regression for two components denoted.

the AlaM treatment. At 60 μg/ml AlaM, addition of Triton X-100 increased the rate from 7.1 ± 0.8 to 9.3 ± 0.1 $\mu mol \cdot min^{-1} \cdot mg^{-1}$ (means $\pm$ S.D. for two independent preparations), indicating diffusion restrictions either in the AlaM pore or through the matrix.

AlaM also makes the inner mitochondrial membrane permeable to NADPH. NADPH-dependent MDH activity (probably also catalysed by the NAD$^+$-MDH; [21]) increased from 10 $nmol \cdot min^{-1} \cdot mg^{-1}$ without AlaM to 68 $nmol \cdot min^{-1} \cdot mg^{-1}$ at 22 μg/ml AlaM. The activity in the presence of Triton X-100 was 113 $nmol \cdot min^{-1} \cdot mg^{-1}$, with or without AlaM (results not shown).

Results show that AlaM makes the inner mitochondrial membrane permeable to NADH and NADPH without affecting the maximum catalytic activity of the enzyme. The higher relative Triton X-100 stimulation of the NADPH-dependent activity when compared with the NADH-dependent activity in the presence of AlaM may suggest a slower movement of NADPH, either through the AlaM pores or through the matrix.

AlaM-treated mitochondria oxidize malate at high rates

The ability of AlaM to empty the matrix of cofactors was investigated by measuring malate oxidation to O_2. Malate oxidation at pH 7.2 engages two matrix enzymes, MDH and NAD$^+$-malic enzyme [23], both reducing NAD$^+$ to NADH. In the absence of added NAD$^+$, malate was oxidized by intact POM at a low rate of 40 $nmol \cdot min^{-1} \cdot mg^{-1}$. Addition of 0.5 mM NAD$^+$ to the assay and the consequent uptake of NAD$^+$ into the matrix [24] led to a modest increase in activity to 54 $nmol \cdot min^{-1} \cdot mg^{-1}$. Addition of AlaM to POM oxidizing malate in state 3 in the absence of added NAD$^+$ instantly abolished malate oxidation (Figure 2). This shows that AlaM caused the immediate loss of NAD$^+$ from the mitochondria. Malate oxidation was restored after NAD$^+$ addition, and an increase in activity to high rates was seen in the AlaM-treated mitochondria with increasing NAD$^+$ added to the medium. AlaM treatment of the mitochondria in the presence of 0.5 mM NAD$^+$ led to an activity approx. 3 times higher than in the control mitochondria (without AlaM), indicating that malate oxidation in intact POM is restricted by the transport of substrates or products into or within the matrix. The concentration dependence for NAD$^+$ was analysed by Eadie–Hofstee plots (Figure 2), which displayed dual components. One component had lower V_{max} and K_m (app), 124 ± 7 $nmol \cdot min^{-1} \cdot mg^{-1}$ and 0.053 ± 0.009 mM respectively. The other component displayed higher V_{max} and K_m, 314 ± 46 $nmol \cdot min^{-1} \cdot mg^{-1}$ and 0.61 ± 0.063 mM respectively (means $\pm$ S.E.M. for three separate mitochondrial preparations).

AlaM allows access to internal NADH dehydrogenases of the respiratory chain

The ETC of plant mitochondria contains at least three NADH dehydrogenases. One, ND_{ex}(NADH), faces the intermembrane space and oxidizes cytoplasmic NADH in a Ca^{2+}-dependent rotenone-insensitive manner. Matrix NADH is oxidized by the rotenone-sensitive complex I and ND_{in}(NADH), both of which are Ca^{2+}-independent [9]. Knowing that AlaM makes the inner mitochondrial membrane permeable to NADH (Figure 1), the accessibility of the internal dehydrogenases to added NADH was investigated in POM using consecutive additions of effectors. EGTA present in the medium will prevent oxidation of added NADH by intact mitochondria. After addition of an agent permeabilizing the inner membrane to NADH (e.g. AlaM), complex I and ND_{in}(NADH) should be active. Addition of rotenone will inhibit complex I, leaving activity via ND_{in}(NADH). After further addition of Ca^{2+}, ND_{ex}(NADH) will also be active.

Various concentrations of AlaM were used to study the effect of AlaM on the oxidation of NADH by the internal NADH dehydrogenases. At low AlaM concentrations, a lag phase was seen with no increase in NADH oxidation (without rotenone or Ca^{2+}) (Figure 3). Further increases in AlaM led to an increase in NADH oxidation, reaching a maximum. A decrease in NADH oxidation was seen at higher AlaM concentrations. This inhibition was strongest at low protein load of POM and not seen at the highest protein load (Figures 3a–3e). In contrast, rotenone-insensitive NADH oxidation via ND_{in}(NADH) increased to a maximum with hardly any decrease at high AlaM concentration for any protein load of mitochondria (Figures 3a–3d). In the presence of Ca^{2+}, the activity showed a transient decrease at low AlaM concentrations (6–12 μg/ml) and also became severely inhibited by high AlaM concentrations (Figures 3a–3d). In Figures 3(f) and 3(g), the rotenone-sensitive part, Δrot (constituting

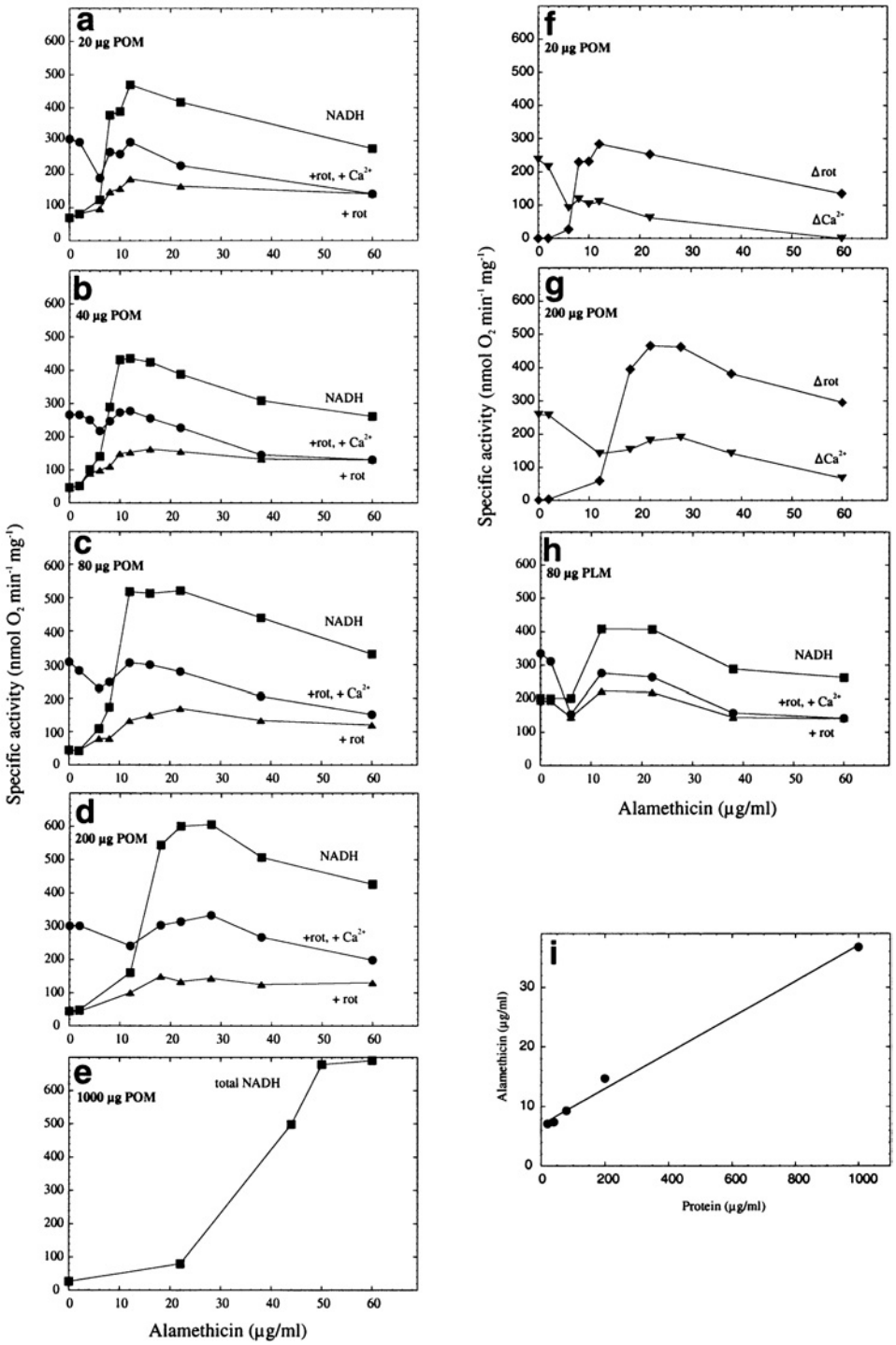

Figure 3 Effect of the concentration of AlaM on the oxidation of NADH at different concentrations of mitochondria

(**a**–**e**) Ca^{2+}-independent NADH oxidation (■), the rate after addition of the complex I inhibitor rotenone (▲) and additionally plus Ca^{2+} (●) by POM at different protein concentrations (μg/ml); (**f**, **g**) the rotenone-sensitive (Δrot; ◆) and the Ca^{2+}-inducible part (ΔCa^{2+}; ▼) for 20 and 200 μg POM protein/ml respectively; (**h**) Ca^{2+}-independent NADH oxidation (■), after addition of the complex I inhibitor rotenone (▲) and additionally plus Ca^{2+} (●) in PLM (PLM) at a concentration of 80 μg of protein/ml; (**i**) the AlaM concentration at half-maximal activity of Ca^{2+}-independent NADH oxidation as a function of protein concentration.

the complex I-linked activity) and the Ca^{2+}-inducible part, ΔCa^{2+} [representing ND_{ex}(NADH)] is presented for 20 and 200 μg of POM protein/ml. A similar pattern of NADH oxidation, was seen for the rotenone-sensitive part (complex I) as for NADH oxidation in the absence of rotenone. The ΔCa^{2+}-dependent activity via ND_{ex}(NADH) decreased biphasically with increasing AlaM. At low protein concentrations, the activity was abolished for high AlaM. Results show that AlaM allows access to internal NADH dehydrogenases of the respiratory chain in POM. Inhibition was seen for Ca^{2+}-independent NADH oxidation at high AlaM

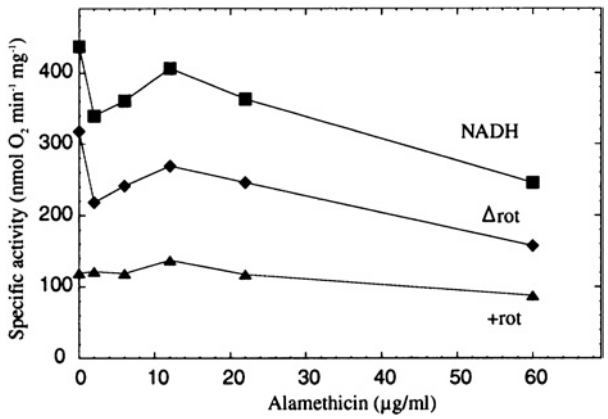

Figure 4 Effect of the AlaM concentration on the oxidation of NADH by IO-SMP

Ca^{2+}-independent NADH oxidation (■), the rate after addition of the complex I inhibitor rotenone (▲) and the rotenone-sensitive part (Δrot; ◆) at an IO-SMP concentration of 80 μg of protein/ml.

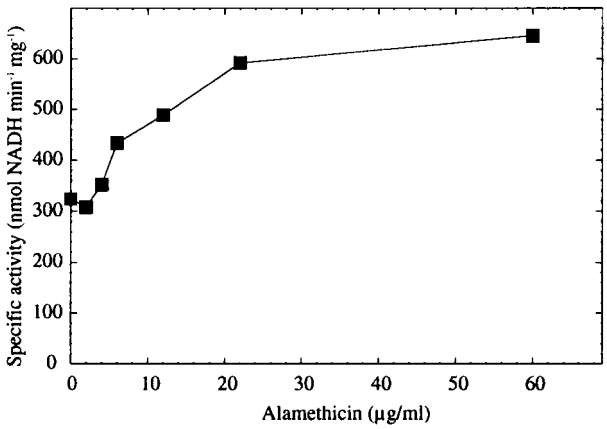

Figure 5 Effect of the AlaM concentration on the oxidation of NADH to DcQ by POM

Ca^{2+}-independent NADH oxidation to DcQ at a mitochondrial concentration of 1 μg/ml.

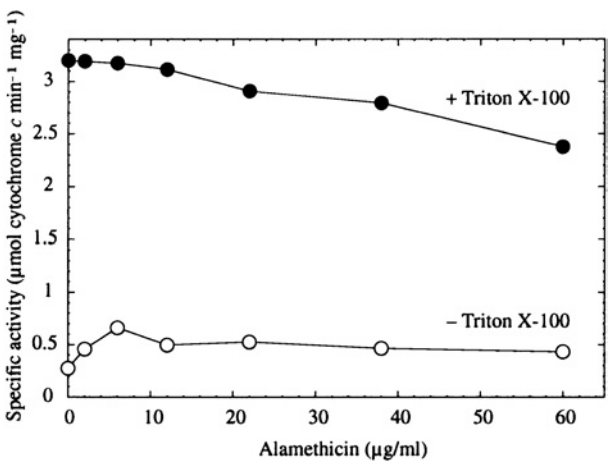

Figure 6 Complex IV activity in POM as a function of AlaM concentration

Activity was determined in the presence (●) or absence (○) of the detergent Triton X-100. The protein concentration in the assay was 1 μg/ml.

concentrations. The ΔCa^{2+} activity was inhibited in a biphasic manner (Figures 3f and 3g).

The concentration of AlaM required to permeabilize the inner membrane, and thus to induce maximum NADH oxidation, was strongly dependent on the concentration of mitochondrial protein (Figures 3a–3e). The amount of AlaM required for maximum NADH oxidation increased from 12 μg of AlaM/ml at 20 μg of protein/ml to 16–22 μg at 80 μg of protein/ml and to 50–60 μg at 1000 μg of protein/ml. When the concentration of AlaM at which half-maximum activity was observed was plotted against the load of mitochondrial protein, a linear relationship was seen (Figure 3i). In addition, the maximum Ca^{2+}-independent NADH oxidation showed an increase with increasing protein concentration from approx. 450 to 700 $nmol \cdot min^{-1} \cdot mg^{-1}$ for 20 μg/ml and 1 mg/ml respectively, indicating that a lower AlaM/protein ratio led to less inhibition of the internal NADH oxidation.

In PLM, the oxidation of exogenously added NADH showed a similar pattern of AlaM effects as for POM: an increasing total rate was observed with increasing AlaM concentrations and decreasing rate at higher AlaM concentrations (Figure 3h). PLM are also very similar to POM in that the ΔCa^{2+} activity shows biphasic inhibition with increasing AlaM concentrations (results not shown). A major difference between POM and PLM was the high Ca^{2+}-independent external NADH oxidation in PLM (200 $nmol \cdot min^{-1} \cdot mg^{-1}$), consistent with previous observations [18].

AlaM inhibits the plant mitochondrial ETC around complexes III and IV and ND_{ex}(NADH)

The inhibition of mitochondrial NADH oxidation activities at both low and high AlaM concentrations gave rise to further experiments to deduce the sites of inhibition. The effect of AlaM on the oxidation of NADH to O_2 by the inner mitochondrial membrane dehydrogenases can be studied directly using IO-SMP. Figure 4 shows NADH oxidation in IO-SMP at a protein load of 80 μg/ml. Inhibition is seen with increasing AlaM concentration, with a transient decrease at low AlaM and a 40 % inhibition at 60 μg/ml AlaM. The rotenone-insensitive NADH oxidation was, however, hardly affected. The inhibition of NADH oxidation in IO-SMP at low and high AlaM concentrations (Figure 4) is similar to the inhibition pattern seen in mitochondria for the Ca^{2+}-induced (Figures 3f and 3g) and Ca^{2+}-independent NADH oxidation (Figures 3a–3d).

The direct effect of AlaM on the internal NADH dehydrogenases can also be studied with DcQ, as an electron acceptor without involving complexes III and IV. In the absence of AlaM, a high rate of external NADH oxidation was observed, consistent with previous observations [25]. The mitochondrial oxidation of NADH to DcQ increased to a maximum after permeabilization with increasing AlaM concentration (Figure 5). No inhibition was seen at high AlaM concentrations, indicating that AlaM inhibition was not due to a direct effect on the Ca^{2+}-independent NADH dehydrogenases.

The effect of AlaM on complex IV, the last step in the cytochrome pathway, was investigated by measuring the oxidation of reduced cytochrome *c*. Figure 6 shows that the oxidation of cytochrome *c* decreased at high AlaM concentrations, leading to an inhibition of 20 % at 60 μg/ml. From the absence of AlaM effects on complex IV activity in the absence of Triton X-100, it can also be seen that AlaM does not make the outer membrane permeable to reduced cytochrome *c*.

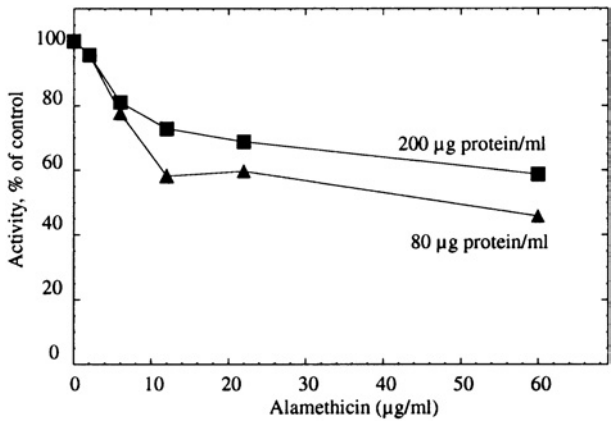

Figure 7 DQH_2 oxidation by POM at two different protein concentrations, 80 (▲) and 200 (■) μg of protein/ml, as a function of AlaM concentration

DQH_2 oxidation is presented as percentage of maximum. Maximum activities were 604 and 402 nmol $\cdot$ min^{-1} $\cdot$ (mg of protein)$^{-1}$ at 80 and 200 μg/ml respectively.

The effect of AlaM on the whole later part of the ETC, including complexes III and IV, was investigated by measuring the oxidation of DQH_2 to O_2. Figure 7 shows DQH_2 oxidation at two concentrations of mitochondrial protein, 80 and 200 μg/ml. In both cases, inhibition was detected at both low and high concentrations of AlaM, although less severe at higher protein load. At 60 μg/ml AlaM for 80 and 200 μg/mg of protein, inhibition was 55 and 40 % respectively.

Succinate oxidation, which bypasses complex I but involves complexes III and IV, was inhibited from 146 to 112 nmol of $O_2 \cdot min^{-1} \cdot mg^{-1}$ by 6 μg/ml AlaM. However, a further increase in AlaM to 22 μg/ml increased the activity to 287 nmol of $O_2 \cdot min^{-1} \cdot mg^{-1}$, indicating that succinate oxidation in unperturbed mitochondria is restricted in succinate or fumarate transport across the inner mitochondrial membrane. At even higher AlaM, succinate oxidation was again inhibited similarly to Ca^{2+}-independent NADH oxidation (results not shown).

Taken together, these results suggest complex III as a site of inhibition at low AlaM concentrations, whereas the additional inhibition at high AlaM concentrations may be due to inhibition of complex IV.

NADH oxidation rates observed in AlaM-treated mitochondria are higher than in IO-SMP and osmotically disrupted mitochondria

Different techniques have been used to get access to and quantify the NADH dehydrogenases on the matrix side of the inner mitochondrial membrane. Therefore NADH oxidation was investigated in and compared between AlaM-treated POM, osmotically disrupted POM and IO-SMP at a protein concentration of 80 μg/ml using an AlaM concentration of 22 μg/ml.

As was observed in Figure 3, a low external Ca^{2+}-independent and rotenone-insensitive NADH oxidation was seen in control mitochondria (Table 1). The external NADH oxidation was highly stimulated by Ca^{2+}. The AlaM-treated mitochondria oxidized NADH at high rates (456 nmol $\cdot$ min^{-1} $\cdot$ mg^{-1} in Table 1, 464 ± 32 on the average for three mitochondrial preparations) in the absence of Ca^{2+}, and this oxidation was inhibited by 70 % by rotenone. NADH oxidation increased after Ca^{2+} addition, engaging ND_{ex}(NADH), but the Ca^{2+}-inducible part was lower compared with that in the control mitochondria. This is consistent with the observed inhibitory effects by AlaM (Figures 3f–3g).

Table 1 NADH oxidation by intact and osmotically burst POM and IO-SMP in the presence or absence of 22 μg/ml AlaM

The activities are presented as specific activity [nmol of $O_2 \cdot min^{-1} \cdot (mg\ of\ protein)^{-1}$] and were measured at a protein concentration of 80 μg/ml. NADH oxidation of burst mitochondria was additionally measured after the addition of 5 μM cytochrome *c*. The rotenone-sensitive (Δrot) and the Ca^{2+}-inducible (ΔCa^{2+}) components are presented in parentheses. Antimycin A-insensitive rates were below 20 nmol of $O_2 \cdot min^{-1} \cdot (mg\ of\ protein)^{-1}$.

		Burst POM		
	Intact POM	Control	+ Cytochrome *c*	IO-SMP
Control				
NADH	47	134	233	334
+ Rotenone	47 (0)	76 (58)	107 (126)	110 (224)
+ Ca	221 (174)	109 (33)	247 (140)	
AlaM				
NADH	456	187	434	324
+ Rotenone	124 (332)	98 (89)	107 (327)	114 (210)
+ Ca	206 (82)	104 (6)	243 (136)	

Osmotic disruption of the mitochondria led to a nearly 3-fold faster Ca^{2+}-independent NADH oxidation compared with intact mitochondria, but the rate was still only approx. one-third of the Ca^{2+}-independent NADH oxidation in the AlaM-treated intact POM. NADH oxidation in osmotically disrupted POM was inhibited by only 40 % by rotenone, and only a small stimulation by Ca^{2+} was seen. Addition of AlaM to the disrupted mitochondria led to some increase in rotenone-sensitive and -insensitive NADH oxidation, but Ca^{2+} stimulation was not retained. The low activities indicated that the osmotic disruption might cause damage to the later part of the ETC. Addition of the mobile carrier cytochrome *c*, which transfers electrons between complexes III and IV, to the disrupted mitochondria increased the rotenone-sensitive, rotenone-insensitive and external Ca^{2+}-dependent NADH oxidation components by 117, 41 and 127 % respectively, compared with the control disrupted mitochondria. Addition of AlaM to the cytochrome *c*-treated disrupted mitochondria led to a further increase in the rotenone-sensitive NADH oxidation component, reaching activities very similar to the activities measured for AlaM-treated intact mitochondria. These results indicate that mitochondria were incompletely disrupted (or were partially resealed after disruption) and that cytochrome *c* was partly released from those mitochondria that were disrupted. This restricted the high total rates of electron transport. In practice, it affected the quantification of activity components measured on top of other activities, i.e. the rotenone-sensitive activity via complex I and the Ca^{2+}-dependent activity via ND_{ex}(NADH). However, the rotenone-insensitive activity via ND_{in}(NADH), measured after inhibition of the other enzymes, was much less perturbed by disruption.

IO-SMP oxidized NADH at a lower rate when compared with the AlaM-treated intact mitochondria, and the activity was unaffected by AlaM treatment. The observed rates in IO-SMP appeared to be low considering that there was a 1.5 times higher complex IV activity in IO-SMP when compared with POM (results not shown), due to loss of matrix proteins after sonication. The lower activity in IO-SMP may reflect damage caused by the IO-SMP preparation procedures (e.g. loss of cytochrome *c* or direct enzyme damage by ultrasonic waves). Adding back cytochrome *c* would have no effect, because the cytochrome *c* binding site is on the inside of IO-SMP.

These results indicate that AlaM provides a better method to quantify internal NADH dehydrogenase activities compared with disruptive techniques such as osmotic bursting and sonication. A

Table 2 Oxidation of NADH, NADPH and DaNADH in POM and IO-SMP in the presence or absence of 22 μg/ml AlaM

Specific activities [nmol of $O_2 \cdot min^{-1} \cdot (mg\ of\ protein)^{-1}$] were measured at a protein concentration of 80 μg/ml. The rotenone-sensitive (Δrot) and the Ca^{2+}-inducible (ΔCa^{2+}) components are presented in parentheses.

	Specific activity	
	Control	AlaM
IO-SMP		
NADH	316	359
+ Rotenone	106 (210)	123 (236)
DaNADH	347	349
+ Rotenone	0 (347)	0 (349)
NADPH	65	61
+ Rotenone	0 (65)	0 (61)
+ Ca	68 (68)	63 (63)
NADPH	65	76
+ Ca	135 (70)	139 (63)
+ Rotenone	71 (64)	78 (61)
POM		
NADH	52	480
+ Ca	299 (247)	537 (57)
+ Rotenone	239 (60)	246 (291)
NADH	51	456
+ Rotenone	47 (4)	141 (315)
+ Ca	240 (193)	241 (100)
DaNADH	16	98
+ Rotenone	0 (16)	0 (98)
NADPH	0	12
+ Ca	108 (108)	107 (95)
+ Rotenone	88 (20)	88 (19)

higher activity with AlaM is seen especially for complex I, but with less difference for the ND_{in}(NADH).

Using AlaM it is possible to obtain information about internal NAD(P)H dehydrogenases in a more natural environment

The properties of NAD(P)H dehydrogenases were investigated on POM and IO-SMP using AlaM. The plant ETC contains Ca^{2+}-dependent rotenone-insensitive NADPH dehydrogenases, one on the outer side and the other on the inner side of the inner mitochondrial membrane [12–15]. NADPH can also be oxidized by plant complex I in a Ca^{2+}-independent manner [12]. DaNADH specifically donates electrons to complex I when using O_2 as electron acceptor [12]. To reach maximum NAD(P)H oxidation, 22 μg/ml AlaM was used at a protein load of 80 μg/ml.

The IO-SMP oxidized NADH and DaNADH at high and similar rates, with no effect by AlaM (Table 2). The DaNADH oxidation was completely inhibited by rotenone, consistent with previous observations [11]. The Δrot activity with NADH was lower when compared with DaNADH. Since both are expected to represent complex I activity, the similar rates of NADH and DaNADH oxidation indicate that the quinol oxidation part of the ETC is saturated, at least during NADH oxidation without rotenone. NADPH oxidation by IO-SMP was measured with consecutive additions of rotenone and Ca^{2+} or in the reverse order. We observed rotenone-sensitive Ca^{2+}-independent NADPH oxidation, representing complex I activity, as well as a Ca^{2+}-dependent activity, as described previously [12]. No effect of AlaM was seen, indicating that there was no contribution by the external NADPH dehydrogenases possibly present on the inner surface of the IO-SMP under these conditions. This is consistent with the release after sonication of NDB proteins, which catalyse external NADPH oxidation and probably NADH oxidation as well [14,26].

NADH oxidation by mitochondria was measured with consecutive additions of rotenone and Ca^{2+} or in the reverse order. A small rotenone inhibition of NADH oxidation in the presence of Ca^{2+} was seen in control mitochondria, which indicates a minor leakage in the inner membrane induced by Ca^{2+} (Table 2).

Complex I-linked activities with different substrates were compared. Virtually no external DaNADH oxidation was seen in intact POM, consistent with previous investigations [11]. After the addition of AlaM, DaNADH oxidation was 20% of the rate of NADH oxidation (98 versus 480 nmol of $O_2 \cdot min^{-1} \cdot mg^{-1}$). The DaNADH activity was totally inhibited by rotenone, confirming that complex I was solely responsible for this activity. However, SMP oxidized DaNADH and NADH at higher and similar rates with no effect of AlaM. These results indicate a difference between NADH and DaNADH in the interaction with complex I studied in AlaM-permeabilized mitochondria but not in IO-SMP. Consistently, with DcQ as acceptor, the rate of DaNADH oxidation was 53% of the rotenone-sensitive NADH oxidation in AlaM-permeabilized mitochondria, but in IO-SMP the corresponding ratio was 111% (results not shown).

NADPH oxidation by intact mitochondria was Ca^{2+} dependent. NADPH oxidation by complex I (Δrot) in AlaM-treated POM was low when compared with the oxidation in IO-SMP, as observed for DaNADH. These results show that complex I substrate specificity is different in IO-SMP and in mitochondria. No AlaM stimulation was seen on the Ca^{2+}-dependent NADPH oxidation, indicating that the internal rotenone-insensitive NADPH dehydrogenase cannot contribute to the NADPH oxidation under these conditions.

DISCUSSION

AlaM permeabilizes plant mitochondria to pyridine nucleotides and dicarboxylic acids

AlaM forms relatively anion-specific voltage-dependent channels in a lipid bilayer when added to its positive side [3]. Respiring mitochondria generate a membrane potential, positive outside, but a lower Donnan potential with the same polarity is maintained even after uncoupling [27]. Thus AlaM channels should also form in the presence of carbonyl cyanide *p*-trifluoromethoxyphenylhydrazone. In recent studies of mammalian and *Yarrowia lipolytica* mitochondria, AlaM channels conducted NADH and other low-molecular-mass hydrophilic compounds [4,5,7,28]. Consistently, AlaM permeabilized the plant mitochondrial inner membrane to NAD(H), NADP(H) and DaNAD(H), oxaloacetate, malate, succinate and fumarate, all negatively charged. The AlaM pore size depends on the number of monomers in each complex, and thus on the AlaM concentration [3]. The lag phase observed at very low AlaM concentrations (2 μg/ml; Figures 1 and 3) most probably represents a state of free AlaM monomers and channels with little or no substrate (e.g. NADH or oxaloacetate) conductance. By increasing the AlaM concentration, substrate-conducting channels are formed, drastically increasing the internal NADH-consuming activities. However, the ability of AlaM to permeabilize mitochondria is also dependent on the AlaM/protein ratio (Figure 3i).

AlaM inhibits the ETC around complexes III and IV and ND_{ex}(NADH)

Depending on substrates and concentrations of AlaM and mitochondrial protein, activities were either stimulated or inhibited by AlaM (Figures 3, 4 and 7). For mammalian mitochondria,

inhibition by AlaM has not been reported. However, AlaM effects have been investigated in a few cases only and without varying protein loads [6,7], hence inhibition may have evaded observation. In plants, the inhibition of NADH oxidation was observed at both low and high concentrations of AlaM (Figures 3, 6 and 7). Antibacterial peptides can inhibit the ETC in plant mitochondria at low concentrations [29], but the mechanism is unknown. In potato, internal NADH to DcQ activity was not inhibited by AlaM, consistent with observations for bovine complex I NADH-Q_1 reductase [5]. By comparing the effects of AlaM on the different steps of the later part of the ETC, we show two sites of inhibition, at low and high concentrations of AlaM, possibly corresponding to inhibition of complexes III and IV respectively. The inhibition of DQH_2 oxidation at low concentrations of AlaM coincides with the observed lag phase in pore formation, indicating that free monomers predominating in this phase inhibit complex III. Inhibition of NADH and DQH_2 oxidation by both low and high concentrations of AlaM was reversed by a high protein/AlaM ratio, and the highest rates of NADH oxidation were measured at the highest protein loads (Figures 3 and 7). AlaM hardly affected the activity of ND_{in}(NADH)-linked NADH oxidation in POM (Figure 3), but the activity via ND_{ex}(NADH) was severely inhibited (Figures 3f and 3g), indicating a direct effect on the dehydrogenase.

NADH oxidation was decreased in IO-SMP at low concentrations of AlaM (Figure 4), but less severely when compared with the inhibition of DQH_2 oxidation (Figure 7). However, at low concentrations, the AlaM would be present at different sides of the inner membrane when assaying POM and IO-SMP, and access different sites of inhibition. The IO-SMP were 90 % inside-out, i.e. 10 % right-side-out, and the latter may have caused the increase in NADH oxidation at higher concentration of AlaM (Figure 4).

Complex I substrate specificities are different in IO-SMP and mitochondria

Complex I can be studied specifically in plants by using the NADH analogue DaNADH as substrate and O_2 as acceptor [11]. Interestingly, we observed that the ratio of DaNADH to NADH oxidation was much lower in the AlaM-permeabilized POM when compared with that in IO-SMP (Table 2). In addition, complex I in IO-SMP oxidizes NADPH, as shown previously [11], but virtually no complex I-linked NADPH oxidation was seen in POM with AlaM. These observations indicate a difference between NADH and DaNADH as well as NADPH in interactions with complex I in the native state inside mitochondria as compared with in IO-SMP. Possibly, this is due to the release of matrix components when producing IO-SMP. It has been suggested that enzymes (e.g. MDH) of the tricarboxylate cycle bind complex I to allow observed shuttling of reducing equivalents inside the matrix (e.g. as malate instead of NADH) [30–32]. It should be noted that most of our knowledge about complex I activity in plants as well as mammals has been obtained by investigating IO-SMP, and the presence of functional associations between complex I and enzymes of the tricarboxylate cycle may have profound consequences for our understanding of respiratory function.

AlaM did not stimulate rotenone-insensitive NADPH oxidation in IO-SMP. Stimulation would be expected, unless the external enzymes are removed from the vesicles by sonication, as suggested by previous studies [26,33–36]. Also, AlaM should not permeabilize IO-SMP, since the membrane potential will be negative outside [3]. In POM, no induction of internal Ca^{2+}-dependent rotenone-insensitive NADPH oxidation by AlaM, on top of the external rate, was seen (Table 2). The Ca^{2+}-ionophore A23187 did not stimulate the NADPH oxidation in AlaM-treated POM (results not shown), suggesting that the lack of induction was not due to a lack of matrix Ca^{2+}. Apart from being present in IO-SMP [11,12], involvement of the internal rotenone-insensitive NADPH dehydrogenase in malate oxidation has been implied in studies on POM and PLM by using the flavoprotein inhibitor diphenyleneiodonium [37,38]. The absence of AlaM stimulation of Ca^{2+}-dependent NADPH oxidation in POM may indicate that the enzyme activity is affected by a matrix protein, which dissociates during sonication, thereby activating the internal NADPH dehydrogenase in IO-SMP. Alternatively, the external and/or internal NADPH dehydrogenase is inhibited by AlaM, similar to the ND_{ex}(NADH) (Figures 3g and 3h).

AlaM empties the matrix of cofactors and allows clamped assay conditions for oxidation of NAD-linked substrates

AlaM-treated plant mitochondria are, as shown in the present study, permeable to low-molecular-mass compounds. Additionally, AlaM has been reported to permeabilize yeast mitochondria to 63–83-residue-long-peptides [39]. In contrast, globular cytochrome *c* with 104 residues does not pass the outer membrane in AlaM-treated POM (Figure 6). Also, mammalian tricarboxylate cycle enzymes are retained in the matrix [5,6]. Thus AlaM pores are small enough to retain the native proteinaceous environment in the matrix while allowing loss and replacement of solutes, peptides and cofactors when studying matrix enzymes and activities.

Addition of AlaM abolished malate oxidation (Figure 2), most probably by releasing endogenous NAD^+ from the mitochondria. In the presence of added NAD^+, control POM accumulate the coenzyme to mM levels [24], suggesting that added AlaM should have stimulated activities (Figure 2) by inducing fast diffusion of substrates and products (malate, oxaloacetate, glutamate, aspartate, pyruvate, adenylates and/or phosphate). In the unperturbed mitochondria, transport would thus impose the major restriction on malate oxidation by limiting the production of NADH for the ETC to oxidize. In AlaM-treated POM, the concentration dependence of malate oxidation for added NAD^+ had dual components. The low-affinity component has a 2-fold higher V_{max} when compared with the high-affinity component, indicating that the two components do not reflect ND_{in}(NADH) and Complex I, where the relative rates are the opposite (Tables 1 and 2). However, under the conditions used, malate is oxidized via both malic enzyme and MDH [23]. The high K_m (app) value is consistent with K_m (NAD^+) value of malic enzyme, which in POM was 0.5–0.9 mM [40], and the low K_m (app) value is also similar to the K_m (NAD^+) value reported for MDH [41], suggesting that the two components reflect these enzymes. However, it should be borne in mind that product inhibition may affect K_m (app) values [42]. On the basis of the mean for three preparations, the total malate oxidation (438 $nmol \cdot min^{-1} \cdot mg^{-1}$) is close to the total internal NADH oxidation under similar conditions (464 $nmol \cdot min^{-1} \cdot mg^{-1}$), i.e. malate oxidation is close to engaging the ETC fully.

AlaM provides a better method to quantify NADH dehydrogenase activities inside the inner membranes

Using the AlaM method, quantification of complex I is best done at a high protein concentration, minimizing inhibition by AlaM, whereas the ND_{in}(NADH)-linked activity can be quantified from small samples (e.g. from tissue treatments). Since ND_{ex}(NADH) can easily be measured in intact mitochondria, the AlaM inhibition of this enzyme is advantageous since it should lead to less interference when assaying internal NADH dehydrogenases.

Disruptive techniques used to study the ETC and quantify the internal NAD(P)H dehydrogenases of plant mitochondria include osmotic burst and the preparation of IO-SMP by sonication. On comparison with AlaM treatment, sonication and osmotic burst especially caused a lower rotenone-sensitive component of NADH oxidation via complex I (Table 1). Major limitations in the activity would be due to incomplete substrate access to the enzyme, loss of cytochrome *c* and direct enzyme damage by ultrawaves. The activities measured on IO-SMP and burst mitochondria, even after the addition of cytochrome *c*, are underestimated. The underestimation will be most severe for high activities (e.g. complex I-linked NADH oxidation), whereas lower activities (e.g. ND_{in}-linked NADH oxidation) are much less affected. In any case, all three methods discussed above give a better estimate of internal NADH dehydrogenase capacities compared with malate oxidation in intact mitochondria (Figure 2).

Conclusions and perspectives

AlaM provides a simple and reliable method to quantify the inner plant mitochondrial dehydrogenases as compared with other methods. The retained mitochondrial ultrastructure, as judged from electron micrographs of mammalian mitochondria [6], and retained proteinaceous environment in the matrix allows investigations of matrix enzymes without potential artifacts due to disruption. A consequence of the latter is exemplified in the present study in the change in substrate specificity for complex I in IO-SMP. Surprisingly, the NADH oxidation rates observed for complex I are much higher than previously known values, i.e. higher than observed with other methods. Here, the complex I-linked activity is 2–3-fold higher than that of succinate and much higher than the oxidation rate of tricarboxylate cycle substrates in isolated mitochondria. In the latter, complex I is limited by a low NADH concentration or NADH:NAD^+ ratio, ultimately caused by restrictions in transport of the substrates.

Depleting mitochondria of cofactors by AlaM treatment allows manipulation of assay conditions and intermediates in the native proteinaceous environment and to clamp effector molecule levels inside the organelle. Therefore AlaM shows great promise for understanding the control of NAD-linked oxidation, but can also be used to modulate other metabolic and molecular processes. Since AlaM preferentially inserts into membranes with a membrane potential positive outside, the method should also work for intact chloroplasts, peroxisomes and cells, with right-side-out-plasma membrane vesicles and inside-out thylakoids.

We are grateful to Dr Hans-Erik Åkerlund for the kind gift of DQH_2. This investigation was supported by grants from the Swedish Research Council for Environment, Agricultural Sciences and Spatial Planning, the Swedish Natural Science Research Council and the Danish Natural Science Research Council.

REFERENCES

1 Douce, R., Aubert, S. and Neuburger, M. (1997) Metabolite exchange between the mitochondrion and the cytosol. In Plant Metabolism (Dennis, D. T., Turpin, D. H., Lefebvre, D. D. and Layzell, D. B., eds.), pp. 234–251, Addison Wesley Longman Ltd, London
2 Cafiso, D. S. (1994) Alamethicin: a peptide model for voltage gating and protein–membrane interactions. Annu. Rev. Biophys. Biomol. Struct. **23**, 141–165
3 Duclohier, H. and Wróblewski, H. (2001) Voltage-dependent pore formation and antimicrobial activity by alamethicin and analogues. J. Membr. Biol. **184**, 1–12
4 Ritov, V. B., Murzakhmetova, M. K., Tverdislova, I. L., Menshikova, E. V., Butylin, A. A., Avakian, T. Y. and Yakovenko, L. V. (1993) Alamethicin as a permeabilizing agent for measurements of Ca^{2+}-dependent ATPase activity in proteoliposomes, sealed membrane vesicles, and whole cells. Biochim. Biophys. Acta **1148**, 257–262
5 Grivennikova, V. G., Kapustin, A. N. and Vinogradov, A. D. (2001) Catalytic activity of NADH-ubiquinone oxidoreductase (complex I) in intact mitochondria – evidence for the slow active/inactive transition. J. Biol. Chem. **276**, 9038–9044
6 Gostimskaya, I. S., Grivennikova, V. G., Zharova, T. V., Bakeeva, L. E. and Vinogradov, A. D. (2003) *In situ* assay of the intramitochondrial enzymes: use of alamethicin for permeabilization of mitochondria. Anal. Biochem. **313**, 46–52
7 Kelley, D. E., He, J., Menshikova, E. V. and Ritov, V. B. (2002) Dysfunction of mitochondria in human skeletal muscle in type 2 diabetes. Diabetes **51**, 2944–2950
8 Rasmusson, A. G., Heiser, V., Zabaleta, E., Brennicke, A. and Grohmann, L. (1998) Physiological, biochemical and molecular aspects of mitochondrial complex I in plants. Biochim. Biophys. Acta **1364**, 101–111
9 Møller, I. M. (2001) Plant mitochondria and oxidative stress: electron transport, NADPH turnover, and metabolism of reactive oxygen species. Annu. Rev. Plant Physiol. Plant Mol. Biol. **52**, 561–591
10 Møller, I. M. and Palmer, J. M. (1982) Direct evidence for the presence of a rotenone-resistant NADH dehydrogenase on the inner surface of the inner membrane of plant mitochondria. Physiol. Plant. **54**, 267–274
11 Rasmusson, A. G. and Møller, I. M. (1991) NAD(P)H dehydrogenases on the inner surface of the inner mitochondrial membrane studied using inside-out submitochondrial particles. Physiol. Plant. **83**, 357–365
12 Rasmusson, A. G. and Møller, I. M. (1991) Effect of calcium ions and inhibitors on internal NAD(P)H dehydrogenases in plant mitochondria. Eur. J. Biochem. **202**, 617–623
13 Melo, A. M. P., Roberts, T. H. and Møller, I. M. (1996) Evidence for the presence of two rotenone-insensitive NAD(P)H dehydrogenases on the inner surface of the inner membrane of potato tuber mitochondria. Biochim. Biophys. Acta **1276**, 133–139
14 Michalecka, A. M., Agius, S. C., Møller, I. M. and Rasmusson, A. G. (2004) Identification of a mitochondrial external NADPH dehydrogenase by overexpression in transgenic *Nicotiana sylvestris*. Plant J. **37**, 415–425
15 Roberts, T. H., Fredlund, K. M. and Møller, I. M. (1995) Direct evidence for the presence of 2 external NAD(P)H dehydrogenases coupled to the electron transport chain in plant mitochondria. FEBS Lett. **373**, 307–309
16 Struglics, A., Fredlund, K. M., Rasmusson, A. G. and Møller, I. M. (1993) The presence of a short redox chain in the membrane of intact potato tuber peroxisomes and the association of malate dehydrogenase with the peroxisomal membrane. Physiol. Plant. **88**, 19–28
17 Day, D. A., Neuburger, M. and Douce, R. (1985) Biochemical characterization of chlorophyll-free mitochondria from pea leaves. Aust. J. Plant Physiol. **12**, 219–228
18 Nash, D. and Wiskich, J. T. (1983) Properties of substantially chlorophyll free pea leaf mitochondria prepared by sucrose density gradient separation. Plant Physiol. **71**, 627–634
19 Arnon, D. I. (1949) Copper enzymes in isolated chloroplasts: polyphenol oxidase in *Beta vulgaris*. Plant Physiol. **24**, 1–15
20 Svensson, Å. S. and Rasmusson, A. G. (2001) Light-dependent gene expression for proteins in the respiratory chain of potato leaves. Plant J. **28**, 73–82
21 Rasmusson, A. G. and Møller, I. M. (1990) NADP-utilizing enzymes in the matrix of plant mitochondria. Plant Physiol. **94**, 1012–1018
22 Møller, I. M., Lidén, A. C., Ericson, I. and Gardeström, P. (1987) Isolation of submitochondrial particles with different polarities. Methods Enzymol. **148**, 442–453
23 Neuburger, M., Day, D. A. and Douce, R. (1984) The regulation of malate oxidation in plant-mitochondria by the redox state of endogenous pyridine nucleotides. Physiol. Veg. **22**, 571–580
24 Tobin, A., Djerdjour, B., Journet, E., Neuburger, M. and Douce, R. (1980) Effect of NAD^+ on malate oxidation in intact plant mitochondria. Plant Physiol. **66**, 225–229
25 Møller, I. M., Roberts, T. H. and Rasmusson, A. G. (1996) Ubiquinone-1 induces external deamino-NADH oxidation in potato tuber mitochondria. Plant Physiol. **112**, 75–78
26 Rasmusson, A. G. and Agius, S. C. (2001) Rotenone-insensitive NAD(P)H dehydrogenases in plants: immunodetection and distribution of native proteins in mitochondria. Plant Physiol. Biochem. **39**, 1057–1066
27 Nicholls, D. G. and Ferguson, S. J. (2002) Bioenergetics 3, p. 54, Academic Press, London
28 Kerscher, S. J., Okun, J. G. and Brandt, U. (1999) A single external enzyme confers alternative NADH: ubiquinone oxidoreductase activity in *Yarrowia lipolytica*. J. Cell Sci. **112**, 2347–2354
29 Hugosson, M., Andreu, D., Boman, H. G. and Glaser, E. (1994) Antibacterial peptides and mitochondrial presequences affect mitochondrial coupling, respiration and protein import. Eur. J. Biochem. **223**, 1027–1033
30 Wiskich, J. T., Bryce, J. H., Day, D. A. and Dry, I. B. (1990) Evidence for metabolic domains within the matrix compartment of pea leaf mitochondria – implications for photorespiratory metabolism. Plant Physiol. **93**, 611–616
31 Millar, A. H., Hill, S. A. and Leaver, C. J. (1999) Plant mitochondrial 2-oxoglutarate dehydrogenase complex: purification and characterization in potato. Biochem. J. **343**, 327–334
32 Srere, P. A. (1993) 17th Fritz Lipmann lecture. Wanderings (wonderings) in metabolism. Biol. Chem. Hoppe Seyler **374**, 833–842

33 Douce, R., Mannella, C. A. and Bonner, W. D. (1973) External NADH dehydrogenases of intact plant mitochondria. Biochim. Biophys. Acta **292**, 105–116
34 Menz, R. I. and Day, D. A. (1996) Identification and characterization of an inducible NAD(P)H dehydrogenase from red beetroot mitochondria. Plant Physiol. **112**, 607–613
35 Luethy, M. H., Thelen, J. J., Knudten, A. F. and Elthon, T. E. (1995) Purification, characterization, and submitochondrial localization of a 58-kilodalton NAD(P)H dehydrogenase. Plant Physiol. **107**, 443–450
36 Rasmusson, A. G., Svensson, A. S., Knoop, V., Grohmann, L. and Brennicke, A. (1999) Homologues of yeast and bacterial rotenone-insensitive NADH dehydrogenases in higher eukaryotes: two enzymes are present in potato mitochondria. Plant J. **20**, 79–87
37 Bykova, N. V. and Møller, I. M. (2001) Involvement of matrix NADP turnover in the oxidation of NAD^+-linked substrates by pea leaf mitochondria. Physiol. Plant. **111**, 448–456
38 Agius, S. C., Bykova, N. V., Igamberdiev, A. U. and Møller, I. M. (1998) The internal rotenone-insensitive NADPH dehydrogenase contributes to malate oxidation by potato tuber and pea leaf mitochondria. Physiol. Plant. **104**, 329–336
39 Venard, R., Brèthes, D., Giraud, M. F., Vaillier, J., Velours, J. and Haraux, F. (2003) Investigation of the role and mechanism of IF1 and STF1 proteins, twin inhibitory peptides which interact with the yeast mitochondrial ATP synthase. Biochemistry **42**, 7626–7636
40 Grover, S. D., Canellas, P. F. and Wedding, R. T. (1981) Purification of NAD malic enzyme from potato and investigation of some physical and kinetic properties. Arch. Biochem. Biophys. **209**, 396–407
41 Heyde, E. and Ainsworth, S. (1968) Kinetic studies on the mechanism of the malate dehydrogenase reaction. J. Biol. Chem. **243**, 2413–2423
42 Hagedorn, P. H., Flyvbjerg, H. and Møller, I. M. (2004) Modeling NADH turnover in plant mitochondria. Physiol. Plant. **120**, 370–385

Received 23 December 2003/11 February 2004; accepted 19 February 2004
Published as BJ Immediate Publication 19 February 2004, DOI 10.1042/BJ20031969